

# Cardiac Current Density Distribution by Electrical Pulses from TASER devices

Robert A. Stratbucker, M.D., Ph.D. \*, Mark W. Kroll, Ph.D. \*\*, Wayne McDaniel, Ph.D. \*\*\* and Dorin Panescu, Ph.D. \*\*\*\*

\* - Stratbucker & Assoc., \*\* - Cal Poly University, San Luis Obispo, CA, \*\*\* - University of Missouri, MO, \*\*\*\* - St. Jude Medical, Sunnyvale, CA

**Abstract — Introduction:** TASERs deliver electrical pulses that can temporarily incapacitate subjects. The goal of this paper is to analyze the distribution of TASER currents in the heart and understand their chances of triggering cardiac arrhythmias.

**Methods and Results:** The models analyzed herein describe strength-duration thresholds for myocyte excitation and ventricular fibrillation induction. Finite element modeling is used to compute current density in the heart for worst-case TASER electrode placement. The model predicts a maximum TASER current density of 0.27 mA/cm<sup>2</sup> in the heart.

**Conclusion:** Numerically simulated TASER current density in the heart is about half the threshold for myocytes excitation and more than 500 times lower than the threshold required for inducing ventricular fibrillation. Showing a substantial cardiac safety margin, TASER devices do not generate currents in the heart that are high enough to excite myocytes or trigger VF.

**Keywords** — Arrhythmia, Modeling, Cardiac, Fibrillation, TASER.

## I. INTRODUCTION

TASERs deliver trains of brief, high-voltage but low-charge electrical pulses designed to temporarily incapacitate subjects through strong neuromuscular activation. They are used as non-lethal weapons by law enforcement personnel to subdue suspects. TASER devices utilize compressed nitrogen to project two small probes up to various ranges of 15, 21, 25 or 35 feet at a speed of over 160 feet per second [1].

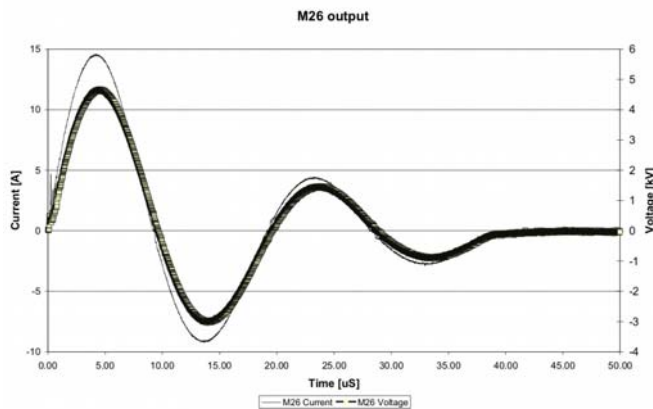


Fig. 1. M26 output for a 400-Ω load.

An electrical signal is transmitted through trailing wires to where the probes make contact with the body or clothing, resulting in an immediate loss of the person's neuromuscular control, with the initial reaction being a gravitational dysreflexia (i.e. fall to the ground), and loss of ability to perform coordinated action for the duration of the impulse. The stimuli from a TASER will override the motor nervous system and block the command and control of the human body. Conventional stun devices stimulate sensory neurons for pain compliance and can be over-ridden by a focused individual. The TASER devices directly stimulate pre-emptive motor nerve tissue, causing incapacitation regardless of subject's mental focus, training, size, or drug induced dementia [1]. The most popular TASER models supplied to law enforcement agencies are the M26 and X26. Their typical output waveforms are shown in Figs. 1 and 2, respectively.

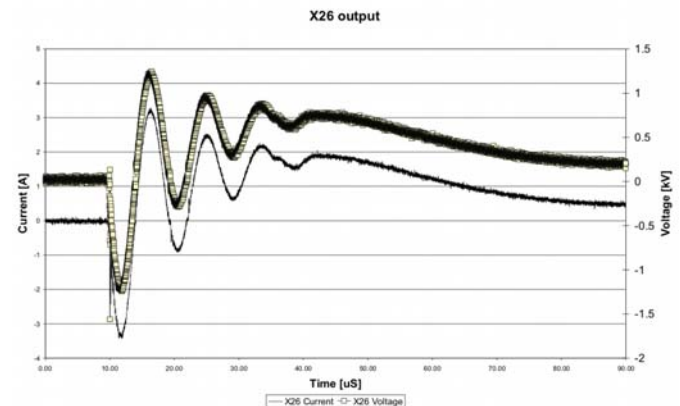


Fig. 2. X26 output for a 400-Ω load.

Table I provides a summary of their specifications.

Table I. Specifications of M26 and X26 TASERs.

Specification	M26	X26
Open-circuit peak voltage [kV]	50	50
Output voltage in typical load [kV]	5	1.2
Rated stored energy [J/pulse]	1.76	0.36
Energy delivered in typical load [J/pulse]	0.5	0.07
Nominal internal power rating [W]	26	7
Power delivered in typical load [W]	10	1.3
Charge in the main phase [μC]	85	100
Pulse rate [pulse/s]	19	19
Total delivery duration [s]	5	5

The M26 delivers a leading biphasic pulse pair of about 10- $\mu$ s duration for each half-cycle. The X26 delivers waveform that to a first approximation appears as a pseudo monophasic (half sinusoid) pulse of about 70  $\mu$ s. The goal of this paper is to analyze the distribution of TASER currents in the heart and understand their chances of triggering cardiac arrhythmias.

## II. METHODS

Previous studies analyzed cardiac safety of TASER devices in animals [4, 5]. For example, Fig. 3 summarizes a very important finding: neuromuscular incapacitating (NMI) electrical discharges, while effective, do not affect the systemic blood pressure [4]. After an average of 26 discharges per animal, all of the nine subject animals remain hemodynamically stable [4].

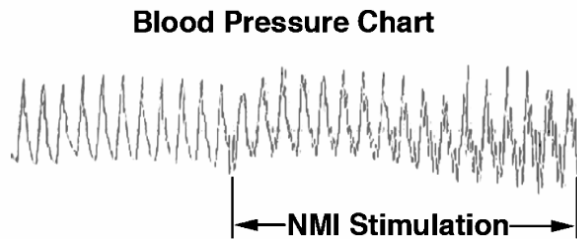


Fig. 3. Blood pressure does not change during application of NMI electric pulses [4].

While this finding addresses to the safety of TASERs from a hemodynamics perspective, it is also important to understand the likelihood of inducing arrhythmic events. Figure 4 shows typical strength-duration curves for current, charge and energy [6].

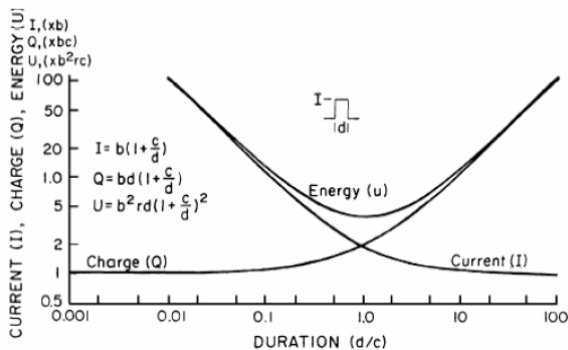


Fig. 4. Strength-duration curves for I, Q and U [6].

Parameter  $c$  represents the chronaxie and equals  $0.693\tau$ , where  $\tau$  is the myocyte membrane time constant. Based on a literature survey, Sun et al. found that the rheobasic current density (i.e. for very long durations – or  $d/c > 10$  in Fig. 4) required to induce ventricular fibrillation (VF) equals  $7 \text{ mA/cm}^2$  [7]. Similarly, they found that the rheobasic current density required to excite myocytes is

$0.12 \text{ mA/cm}^2$ . As presented in Figs. 1 and 2, the longest duration of the main phase TASER current is about 70  $\mu$ s, for the X26 model. The myocyte chronaxie is about 0.2 ms, for an excitation model, and 1.2 ms, for a VF induction model [6, 7]. The corresponding  $d/c$  values are 0.35 and 0.05, for excitation and VF, respectively. Therefore, using Fig. 4, the corresponding current density thresholds required to excite myocytes and to induce VF are about  $0.5 \text{ mA/cm}^2$  and  $140 \text{ mA/cm}^2$ , respectively. In order to understand how this range of current densities compares to currents induced in the heart by TASER discharges, we present a finite element model (FEM) of the human body. Figure 5 shows the FE mesh. The FEM includes the following tissue regions:

- Muscle (neck, shoulder, limbs)
- Bone (spine, ribcage)
- Heart
- Lungs
- Skin/Fat
- Abdomen

The model consists of 8640 hexahedral elements.

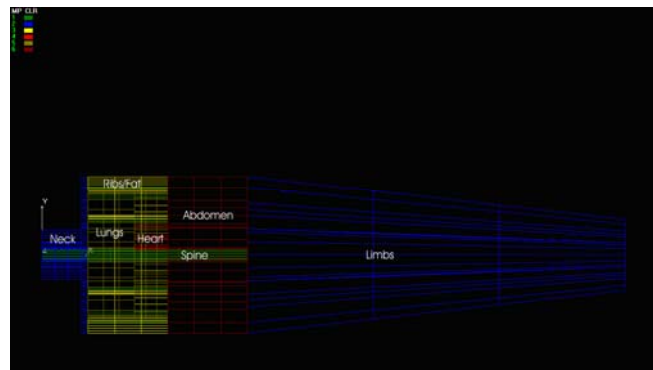


Fig. 5. The FE mesh includes 7 regions.

Tissue resistivities are assigned using values published in previous work [8]. To simulate worst-case scenario, the probe electrodes are placed at chest locations over the heart, approximately 7 cm apart. This is the minimal TASER probe separation and it is seen in drive stun mode. Voltage type boundary conditions are set at nodes corresponding to the assumed probe placement. Given that Cosmos, the FE software used in this study, solves for steady state, rather than the transient solutions, the applied voltage is set at 100 V. This boundary condition is in the range of rms voltages delivered with by TASER devices. This range can be computed by multiplying the current rms range from Table I by the range of typical tissue impedances seen during probe deployment. Thus, the range is:  $151\text{-}162 \text{ mA}_{\text{rms}} * 500\text{-}1000 \Omega = 75.5 - 162 \text{ V}$  [2, 3].

### III. RESULTS

Figures 6 and 7 show the voltage and current density distributions predicted by the FE solver. The voltage in the model reaches its maximum in the electrode region. Then, it decreases rapidly with distance from electrode. Similarly, the current density reaches its maximum in the tissue region beneath electrodes then it decreases rapidly. The maximum current density at the elements representing the heart is  $0.27 \text{ mA/cm}^2$ .

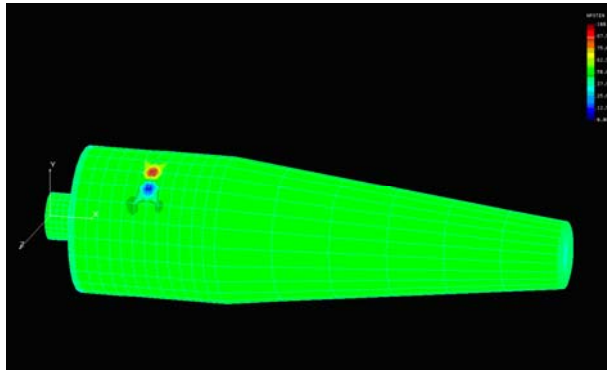


Fig. 6. FEM voltage distribution in V.

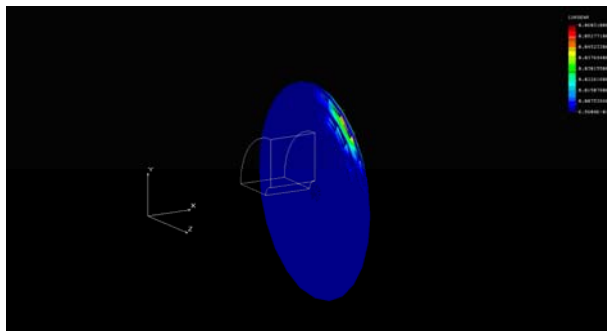


Fig. 7. FEM current density distribution in the heart expressed in  $\text{A/cm}^2$ .

The FEM assumes an electrical resistivity of the heart region of  $450 \text{ } \Omega\text{-cm}$  [8]. Based on these numbers, the corresponding maximum electric field strength in the heart is approximately  $0.12 \text{ V/cm}$ .

### IV. CONCLUSIONS

The maximum TASER current density in the heart,  $0.27 \text{ mA/cm}^2$ , is about half  $0.5 \text{ mA/cm}^2$ , the threshold required to excite myocytes, and more than 500 times lower than  $140 \text{ mA/cm}^2$ , the threshold required to induce VF. These numbers can also be analyzed from an electric field strength perspective. The myocyte excitation threshold is reported to be between  $2\text{-}5 \text{ V/cm}$  [9, 10]. Compared to the lower end of the interval,  $2 \text{ V/cm}$ , the maximum TASER electric field strength in the heart,  $0.12 \text{ V/cm}$ , is significantly lower than the threshold required for initiating cardiac rhythm

disturbances. Showing a substantial cardiac safety margin, even under worst-case probe placement, TASER devices do not generate currents in the heart that are high enough to excite myocytes or trigger VF.

### V. REFERENCES

- [1] TAER International: *TASER Technology Summary*. Available at <http://www.taser.com/facts/qa.htm>
- [2] TASER International, *Advanced TASER: M-Series Operating Manual*. 2005.
- [3] TASER International, *Advanced TASER: X-Series Operating Manual*. 2005
- [4] W. McDaniel, R. A. Stratbucker, M. Nerheim, and J. E. Brewer, "Cardiac safety of neuromuscular incapacitating defensive devices," *PACE*, vol. 28, pp. S1-S4, 2004.
- [5] W. McDaniel, R. A. Stratbucker, and R. W. Smith, "Surface application of Taser stun guns does not cause ventricular fibrillation in canines," *Proc. IEEE-EMBS Ann. Intl. Conf.*, 2000.
- [6] L.A. Geddes and L.E. Baker: 'Principles of Applied Biomedical Instrumentation', 3rd ed., John Wiley & Sons, New York, pp. 460, 1989.
- [7] H. Sun, J.-Y. Wu, R. Abdallah, and J. G. Webster, "Electromuscular incapacitating device safety," *Proc. IFMBE*, vol. 11(1), 3<sup>rd</sup> EMBE Conference, Prague, 2005.
- [8] D. Panescu, J. G. Webster, W. J. Tompkins and R. A. Stratbucker, "Optimization of cardiac defibrillation by three-dimensional finite element modeling of the human thorax," *IEEE Trans. Biomed. Eng.*, vol. 42, no. 2, pp. 185-192, 1995.
- [9] S. B. Knisley, W. M. Smith and R. E. Ideker, "Effect of field stimulation on cellular repolarization in rabbit myocardium. Implications for reentry induction," *Circ Res.*, vol. 70(4), pp. 707-715, 1992.
- [10] S. B. Knisley, W. M. Smith and R. E. Ideker, "Prolongation and shortening of action potentials by electrical shocks in frog ventricular muscle," *Am. J. Physiol.*, vol. 266(6 Pt 2), pp. H2348-2358, 1994.